*Journal of Thermal Analysis and Calorimetry, Vol. 90 (2007) 1, 185–189*

# CRYSTALLIZATION OF SPODUMENE-DIOPSIDE IN THE LAS GLASS CERAMICS WITH CaO AND MgO ADDITION

*A.-M. Hu*, M. Li and D.-L. Mao*

School of Materials Science and Engineering, The State Key Laboratory of the Metal Matrix Composites, Shanghai Jiaotong University, 1954 Huashan Road, Shanghai 200030, P. R. China

Crystallization, morphology and mechanical properties of a spodumene-diopside glass ceramics with adding different amount of CaO and MgO in $Li_2O$–$Al_2O_3$–$2SiO_2$ were investigated. With CaO and MgO addition, the crystallization temperature ($T_p$) decreased, the value of Avrami constant ($n$) decreased from 3.2±0.3 to 1.4±0.2, the activation energy ($E$) increased from 299±3 kJ mol$^{-1}$ to 537±5 kJ mol$^{-1}$. The crystalline phases precipitated were *h*-quartz solid solution, β-spodumene and diopside. The mechanism of crystallization of the glass ceramics changed from bulk crystallization to surface crystallization. The grain sizes and thermal expansion coefficients increased while the flexural strength and fracture toughness of the glass-ceramics increased first, and then decreased. The mechanical properties were correlated with crystallization and morphology of glass ceramics.

***Keywords:*** *crystallization, glass, glass-ceramics, grain growth, mechanical properties*

## Introduction

Glass-ceramics had been investigated for more than three decades. It is important to design the composition and control the crystallization of the glass to achieve desired microstructure and properties [1–3]. Lithium aluminosilicate (LAS) glass-ceramics had gained considerable attention because of their very low thermal expansion coefficient (CTE), high transparency, excellent thermal shock resistance and chemical durability [1–4]. In LAS glass-ceramics, the ultralow thermal expansion is duo to the main crystalline phases: high-quartz solid solution ($Li_2O$–$Al_2O_3$–$2SiO_2$) and β-spodumene ($Li_2O$–$Al_2O_3$–$4SiO_2$), but there are some shortage: they have low strength (100 MPa for high-quartz and 140 MPa for β-spodumene), and need high melting temperature (above 1873 K) to produce the glass ceramics. To lower the melting temperature, some fluxes such as alkali oxides, alkali earth oxides, Lanthanon metal oxides, $B_2O_3$, $P_2O_5$ and $F^-$ had been added in LAS glass ceramics for many years [5–15]. But these additives can not solve the problems of lower strength at the same time. Diopside glass ceramics ($CaO{\cdot}MgO{\cdot}2SiO_2$) has higher bending strength (300 MPa) and fracture toughness (3.5 MPa m$^{1/2}$) [16–21]. Ashizuka had reported that in $CaO$–$MgO$–$SiO_2$–$P_2O_5$ system with diopside and apatite as main phase, the glass–ceramics had high strength (about 236 MPa) [17], much higher than only apatite (about 100 MPa). It is desired to produce a glass ceramics with two phases: spodumene and diopside, this glass ceramics will have low thermal expansion and high mechanical properties.

In this work, different amount of CaO+MgO were added in LAS glass to obtain high strength and low melting temperature glass ceramics with diopside and spodumene as main phase, and the crystallization, morphology and mechanical properties of a spodumene-diopside glass ceramics were investigated.

## Theory background

The kinetics of crystal growth in glass can be investigated using the Johnson-Mehl-Avrami (JMA) equation [22–28]:

$$-\ln(1-x) = (kt)^n \quad (1)$$

where $x$ is the volume fraction of crystallized phase at time $t$, $n$ is the Avrami exponent related to the mechanism of crystallization, and $k$ is the reaction rate constant, related to the absolute temperature $T$, by Arrhenius type equation:

$$k = \nu \exp\left(-\frac{E}{RT}\right) \quad (2)$$

where ν is the frequency factor, $R$ is the gas constant and $E$ is activation energy of crystal growth. The reaction rate constant $k$ can also express as [24]:

$$k = AN \exp(-E/RT) \quad (3)$$

* Author for correspondence: huanmin@tsinghua.org.cn

*1388–6150/$20.00*

*Akadémiai Kiadó, Budapest, Hungary*
*Springer, Dordrecht, The Netherlands*

$A$ is a constant, and the number of nuclei per unit volume, $N$, in a glass $N$ can be expressed as [29]:

$$N = N_s+N_h+N_n+N_c \quad (4)$$

where, $N_s$ is the number of surface nuclei per unit volume, $N_h$ is the number of bulk nuclei formed during a DTA scan per unit volume, $N_n$ is the number of nuclei formed during a previous heat treatment, and $N_c$ is the number of heterogeneous bulk nuclei per unit volume. The values of $N_s$ are proportional to the sample specific surface, $S$, and the reciprocal of DTA heating rate, the time of the nucleation heat treatment and the amount of nucleating agent, respectively. The samples with small particle size mean large values of $N_s$, $N_h$, $N_n$ and $N_c$.

The relationship between the number of nuclei per unit volume, $N$, and $T_p$ can be described as [29, 30]:

$$\ln(N) = E/RT_p+\ln\alpha+C \quad (5)$$

where $\alpha$ is the heating rate of DTA. According to Eq. (5), it can also find that increasing the concentration of nuclei causes a shift of the peak towards lower temperatures and vice versa. This means that the crystallization peak temperature $T_p$ decreased with smaller particle size [29, 30]. Tosic [29] found that the shift of crystallization peaks $T_p$ with different heating rates for powdered glass particles <0.038 and 0.5–0.7 mm was about 50°C.

Developed from Eqs (1) and (2), non-isothermal crystallization kinetics of glass can be described by the expression [22–24]:

$$\ln\frac{T_p^2}{\alpha} = \frac{E}{RT_p}+C \quad (6)$$

The Avrami parameter $n$=1 indicates mono-dimensional growth (surface crystallization), $n$=2 indicates two-dimensional crystallization, and $n$=3 implies bulk crystallization [25–33]. $E$ is the activation energy of crystal growth. Values of $E$ can be calculated by Eq. (6) by plots of $\ln(T_p^2/\alpha)$ *vs.* $1/T_p$.

The value of $n$ can be calculated by the Augis-Bennett equation [34]:

$$n = \frac{2.5}{\Delta T}\frac{RT_p^2}{E} \quad (7)$$

where $\Delta T$ is the full width of the exothermic peak at half maximum intensity (FWHM).

## Experimental

### *Materials*

The starting materials were analytical grade: $SiO_2$, $Al_2O_3$, MgO, $Li_2CO_3$, $CaCO_3$, ZnO and $TiO_2$ and the detailed proportions of the glasses were given in Table 1. Glass batches were melted in alumina crucibles at 1773~1873 K for 2 h according to the composition to obtain homogeneous, transparent glasses from all compositions, then annealed at 873 K for 1 h.

**Table 1** Composition of the glasses (mass%)

| Sample | $Li_2O$ | $Al_2O_3$ | $SiO_2$ | MgO | CaO | $TiO_2$ |
|---|---|---|---|---|---|---|
| 1 | 4.5 | 16.3 | 69.5 | 1.2 | 1.5 | 7.0 |
| 2 | 4.3 | 15.7 | 66.4 | 3.0 | 3.6 | 7.0 |
| 3 | 4.0 | 14.4 | 61.5 | 6.1 | 7.0 | 7.0 |
| 4 | 3.7 | 13.8 | 59.2 | 7.5 | 8.8 | 7.0 |

### *Methods*

Differential thermal analysis (DTA) of annealed glass specimens were carried out in a Dupont 2100 Thermal Analyzer. The quenched glasses were ground and screened to four different particle sizes: <20, 38~63, 100~160 and 200~315 μm. These different particle sizes ranges were designated as: 20, 50, 100 and 200 μm. Non-isothermal experiments were performed by heating 30 mg samples in a Pt crucible with $Al_2O_3$ as the reference material in the temperature range between 293 and 1473 K at 5~20 K $min^{-1}$ under a flowing atmosphere of drying air (30 $cm^3$ $min^{-1}$).

X-ray diffraction (XRD) investigations were done with a D-max-RB diffractometer with $CuK_\alpha$ radiation ($\lambda_{K\alpha1}$ = 0.15406 nm) operating at 35 kV and 40 mA in the 2θ range from 10 to 70° at 0.02° steps.

Scanning electron microscopy (SEM) was conducted with a JSM-6301F. Specimens were prepared with standard metallographic techniques followed by chemical etching in an HF solution (5%) for 90 s. Etched glass–ceramic samples were coated with a thin layer of gold.

The strength of the samples were measured in ten specimens for each sample (4×3×36 mm) using a 4-point bending strength with a span of 30 mm at a crosshead speed of 0.5 mm per 60 s. The fracture toughness were measured by an indentation fracture (IF) method using the Evans equation to calculate $K_{IC}$ from the length of the crack and the semi-diagonal of the indentation [35].

## Results and discussion

### *DTA results*

DTA curves for the four glass samples with particle sizes 200 μm at a heating rate of 10 K $min^{-1}$ are shown in Fig. 1. As the CaO, MgO can serve as network modifiers to reduce the melting point and viscosity of

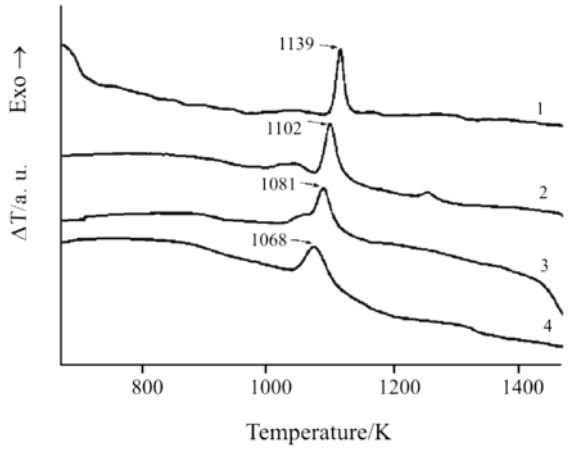


**Fig. 1** DTA curves of glass samples, $\alpha$=10 K min$^{-1}$

the glass; it can see from Fig. 1 that with more CaO+MgO addition, the glass crystallization peak temperatures decrease, from 1139 to 1068 K.

The values of $E$ can calculate by Eq. (6) by plots of $\ln(T_p^2/\alpha)$ *vs.* $1/T_p$ which are shown in Fig. 2, the results are given in Table 2. With more CaO and MgO addition, the activation energy of crystal growth $E$, corresponding to the energy barrier of transition from glass to crystal, increases from 299 kJ mol$^{-1}$ to 537 kJ mol$^{-1}$, this means that the glass is difficult to crystallization by CaO and MgO addition.

The values of $n$ calculated by Eq. (7) for four glasses are 3.2, 2.6, 1.9, 1.4, and the results are given in Table 2, this means the crystallization mechanism change from bulk to surface crystallization with more CaO+MgO addition.

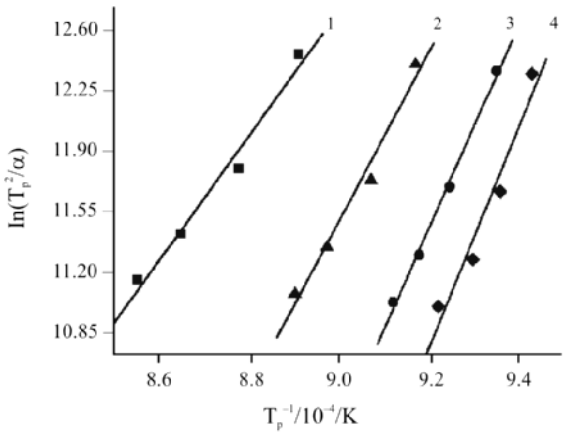


**Fig. 2** Plots of $\ln T_p^2/\alpha$ *vs.* $1/T_p$ for the four glasses

**Table 2** The values of activation energy $E$, Avrami parameter $n$ and the crystallization peak temperatures $T_p$

| No. | 1 | 2 | 3 | 4 |
|---|---|---|---|---|
| $E$/kJ mol$^{-1}$ | 299±3 | 403±4 | 485±3 | 537±5 |
| $n$ | 3.2±0.3 | 2.6±0.2 | 1.9±0.3 | 1.4±0.2 |
| $T_p$/K | 1139 | 1102 | 1081 | 1068 |

**Table 3** Crystallization peak temperature (K) for the glass samples with different particle size, $\alpha$ = 10 K min$^{-1}$

| Sample | Crystallization peak temperature/K | | | | $\delta T$/K |
|---|---|---|---|---|---|
| | Particles size/μm | | | | |
| | 200 | 100 | 50 | 20 | |
| 1 | 1139 | 1135 | 1133 | 1132 | 7 |
| 2 | 1102 | 1093 | 1085 | 1078 | 24 |
| 3 | 1081 | 1069 | 1061 | 1050 | 31 |
| 4 | 1068 | 1051 | 1040 | 1024 | 44 |

The crystallization peak temperatures for the glasses with different particle sizes are shown in Table 3, where, $\delta T$ values are the peak temperatures differences between particle size 200 and 20 μm. From Table 3, as the particle size decrease from 200 to 20 μm, all crystallization peak temperatures shift to lower temperature [29, 30], but there are differences. The sample No. 1 has the smallest $\delta T$, and the value of $\delta T$ is 7 K; while the sample No. 4 has the largest $\delta T$, the value of $\delta T$ is 44 K. This means that the value of $T_p$ in the bulk crystallization is less affected by the change of the particle size, while $T_p$ in the surface crystallization is more affected by the particle size. Alizadeh [36] also found that in the MgO–CaO–$SiO_2$–$Na_2O$ glass system, the bulk crystallization samples had the smaller $\delta T$, while, the surface crystallization glass had larger $\delta T$. This phenomenon is also seen in this study.

*XRD results*

The powder XRD patterns of the glasses heat-treated at 1073 K for 2 h are shown in Fig. 3. *h*-quartz solid solution appears in all samples. XRD results indicate that with CaO+MgO addition, the first phase appeared is still *h*-quartz solid solution. With more CaO and MgO addition, such as sample 3 and 4, a few

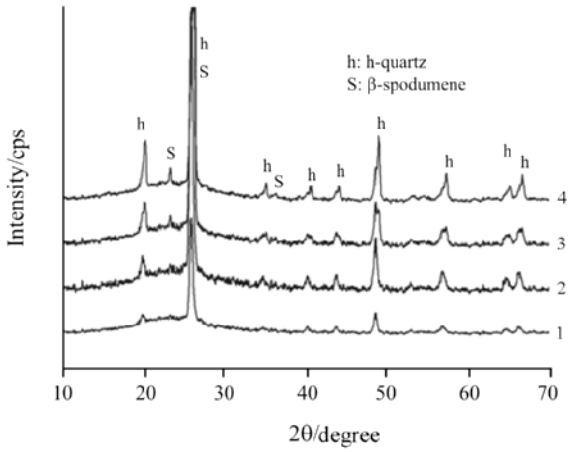


**Fig. 3** XRD patterns of the glass-ceramics samples heat-treated at 1073 K/2 h

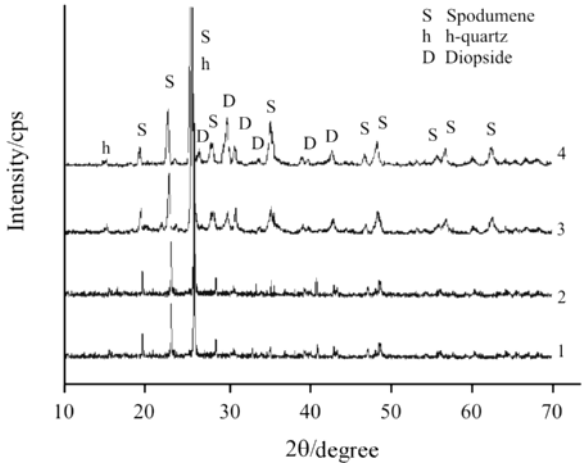


**Fig. 4** XRD patterns of the glass-ceramics samples heat-treated at 1323 K/2 h

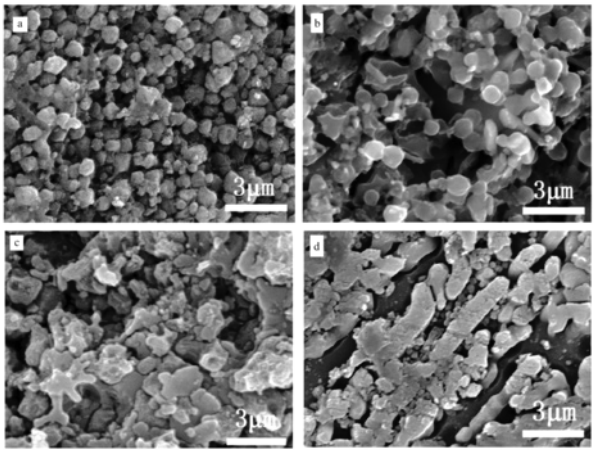


**Fig. 5** SEM photographs of a-1, b-2, c-3 and d-4 samples; heat-treated at 1323 K for 2 h

β-spodumene appears besides *h*-quartz solid solution. Figure 4 illustrates the powder XRD patterns of the glasses heat-treated at 1323 K for 2 h. As in Sample 1 and 2, the main phase was β-spodumene, no diopside appeared. CaO and MgO may enter into the *h*-quartz or β-spodumene structure. With more CaO+MgO addition, as in samples 3 and 4, the phase of diopside increased at the expense of β-spodumene. A trace of *h*-quartz solid solution still appeared in all samples.

*Microstructures*

Figure 5 shows SEM micrographs of the glass–ceramic samples heat-treated at 1323 K for 2 h. Samples 1 and 2 have homogeneous dispersion of tiny spherical crystallites, the grain sizes were 1–2 μm (Figs 5a and b). These indicate that the crystallization mechanism is bulk crystallization. With more CaO+MgO addition, as in sample 3, there are plate-like crystals instead of tiny spherical crystals, and the grain sizes increase to about 3–4 μm. With even more CaO+MgO addition, as in samples 4, the crystallization is observed to start at surface of the glasses sample, then proceeds towards the interior of the glass matrix, and show coarse dendritic in shape. These results are in agreement with the above crystallization kinetics analysis that crystallization mechanism change from bulk crystallization to surface crystallization with CaO+MgO addition.

*Thermal expansion and bending strengths*

After crystallization at 1323 K for 2 h, the mechanical properties of four glass-ceramics are given in Table 4. With more CaO+MgO addition, diopside increase at the expense of β-spodumene (CTE is $3\sim9\cdot10^{-7}\,K^{-1}$) [1–5], as diopside has high positive thermal expansion coefficients (CTE is $50\sim150\cdot10^{-7}\,K^{-1}$) [15], the thermal expansion coefficients increase.

The values of Vickers hardness, elastic moduli, flexural strength and fracture toughness have different trends and the sample 3 has the maximum values. The properties of glass ceramics are correlated with crystallization and morphology. After crystallization at 1323 K/2 h, the main phase of sample 1 is β-spodumene, so the samples have almost the same properties as pure β-spodumene with a flexural strength about 140 MPa [1–3]. With more CaO+MgO addition, as in sample 3, spodumene-diopside glass ceramics with the morphology of the interlock plate-like grains is obtained. As diopside have higher flexural strength (300 MPa) [16–18], and the randomly oriented and interlocked plate spodumene-diopside crystallites, which cause crack divert or blunt to limit the further development of the flaw size and increase the surface energy of

**Table 4** The mechanical properties of spodumene-diopside glass-ceramics heat treated at 1323 K for 2 h

| Sample | The Vickers hardness/GPa | Elastic moduli/GPa | Flexural strength/MPa | Fracture toughness/ MPa $m^{1/2}$ | Expansion coefficient/K | Thermal shock resistance*/°C |
|---|---|---|---|---|---|---|
| 1 | 6.3 | 91 | 138 | 1.6 | $7.4\cdot10^{-7}$ | 800 |
| 2 | 6.2 | 87 | 144 | 1.7 | $9.9\cdot10^{-7}$ | 810 |
| 3 | 6.8 | 93 | 197 | 2.9 | $11.8\cdot10^{-7}$ | 920 |
| 4 | 6.4 | 89 | 152 | 1.9 | $19.3\cdot10^{-7}$ | 720 |

*(in 20°C water)

fracture, so, high flexural strength values (199 MPa) can obtain [18, 37]. In sample 4, although more diopside is precipitated in the glass ceramics, the coarse dendritic grains can increase the further development of the flaw which will lower the mechanical properties [37].

## Conclusions

Spodumene-diopside glasses ceramics were obtained with CaO+MgO addition. As CaO+MgO content increased, the crystallization temperature decreased, and the crystallization of the glass ceramics changed from bulk crystallization to surface crystallization, the grain sizes and thermal expansion coefficients increased, while the flexural strength and fracture toughness of the glass-ceramics reached the maximum value with 6.1% MgO+7.0% CaO addition. The mechanical properties were correlated with crystallization and morphology of glass ceramics.

## References


1 G. H. Beall and L. R. Pinckney, J. Am. Ceram. Soc., 82 (1999) 5.
2 L. Arnault, M. Gerland and A. Riviere, J. Mater. Sci., 35 (2000) 2331.
3 A. M. Hu, K. M. Liang, G. L. Wang and F. Zhou, J. Therm. Anal. Cal., 78 (2004) 991.
4 M. Guedes, A. C. Ferro and J. M. F. Ferreira, J. Eu. Ceram. Soc., 21 (2001) 1187.
5 A. M. Hu, K. M. Liang, P. Fei and F. Zhou, Thermochim. Acta, 413 (2004) 53.
6 C. Leonelli, T. Manfredini and M. Paganelli, J. Am. Ceram. Soc., 74 (1991) 983.
7 M. C. Wang, M. H. Hon and F. S. Yen. J. Cryst. Growth, 91 (1988) 155.
8 K. J. Anusavice and N. Z. Zhang, J. Am. Ceram. Soc., 80 (1997) 1353.
9 J. J. Shyu and M. T. Chiang, J. Am. Ceram. Soc., 83 (2000) 635.
10 K. Davkova, S. Zafirovski, S. Pocev and V. Zlatanovic, Glass Technology, 41 (2000) 197.
11 J. J. Shyu and C. S. Hwang, J. Mater. Sci., 31 (1996) 2631.
12 M. H. Lin and M. C. Wang, J. Mater. Res., 11 (1996) 2611.
13 L. Barbieri, A.B. Corradi, C. Leonelli, C. Siligardi, T. Manfredini and G. C. Pellacani, Mater. Res. Bull., 32 (1997) 637.
14 J. Ma. Rincón, M. Romero, J. Marco and V. Caballer, Mater. Res. Bull., 33 (1998) 1159.
15 A .W. A. Elshennawi, E. M. A. Hamzawy, G. A. Khater and A. A. Omar, Ceram. Int., 27 (2001) 725.
16 H. Anmin, L. Ming and M. Dali, J. Therm. Anal. Cal., 84 (2006) 497.
17 M. Romero, J. Ma. Rincón and A. Acosta, J. Eur. Ceram. Soc., 22 (2002) 883.
18 M. Ashizuka and E. Ishida, J. Mater. Sci., 32 (1997) 185.
19 P. Alizadeh and V. K. Marghussian, J. Eur. Ceram. Soc., 20 (2000) 765.
20 R. Cio, P. Pernice, A. Aronne and G. Quattroni, J. Mater. Sci., 28 (1993) 6591.
21 E. M. Kucukbayrak, S. Ersoymericboyu and M. L. Aovecoglu, J. Eur. Ceram. Soc., 21 (2001) 2835.
22 H. E. Kissinger, J. Res. Nat'l Bureau Stand., 57 (1956) 217.
23 M. Avrami, J. Chem. Phys., 9 (1939) 177.
24 W. A. Johnson and K. F. Mehl, Trans. AIME., 135 (1939) 416.
25 M. Ciecinska, J. Therm. Anal. Cal., 84 (2006) 201.
26 J. Pospisil, P. Mosner and L. Koudelka, J. Therm. Anal. Cal., 84 (2006) 479.
27 M.A. Aksan, M. E. Yakinci and Y. Balci, J. Therm. Anal. Cal., 81 (2005) 417.
28 E. Jona, P. Simon, K. Nemcekova, V. Pavlik, G. Rudinska and E. Rudinska, J. Therm. Anal. Cal., 84 (2006) 673.
29 R. G. Duan, K.M.Liang and S. R. Gu, J. Eur. Ceram. Soc., 18 (1998) 1729.
30 M. B. Tošić, M. M. Mitrović and R. Ž. Dimitrijević, J. Mater. Sci., 35 (2000) 3659.
31 Y. J. Park and J. Heo, Ceram. Int., 28 (2002) 669.
32 Y. K. Lee and S. Y. Choi, J. Mater. Sci., 32 (1997) 431.
33 R. Iordanova, E. Lefterova, I. Uzunov, Y. Dimitriev and D. Klissurski, J. Therm. Anal. Cal., 70 (2002) 393.
34 J. A. Augis and J. E. Bennett, J. Thermal Anal., 13 (1978) 283.
35 A. M. Hu, M. Li, D. L. Mao and K. M. Liang, Thermochim. Acta, 437 (2005) 110.
36 P. Alizadeh and V. K. Marghussian, J. Mater. Sci., 35 (2003) 1529.
37 W. Holand, V. Rheinberger and M. Frank, J. Non-Crystal. Sol., 253 (1999) 170.


Received: July 5, 2006
Accepted: November 7, 2006
OnlineFirst: February 26, 2007

DOI: 10.1007/s10973-006-7795-8